An evaluation of Contrast-to-Noise Ratios for Diffusion Anisotropy Metrics in the presence of Multiple Fibres

M. M. Correia[1], V. F. Newcombe[1], T. A. Carpenter[1], and G. B. Williams[1]
[1]Wolfson Brain Imaging Centre, University of Cambridge, Cambridge, United Kingdom

Introduction

Despite the undeniable successes of *FA* (fractional anisotropy), DTI derived anisotropy metrics can be inaccurate in the presence of orientational heterogeneity. In this case, using the 2-rank tensor model gives rise to an excessive smoothing of the diffusivity profile, hence a reduction in the anisotropy value. Many alternative indices have been proposed from simple modifications to *FA* to highly complex new model approaches. Several studies have compared the indices calculated directly from the eigenvalues of the diffusion tensor (e.g. [1-3]). However, less attention has been given to more complicated metrics, and may of them have never been used in clinical studies. The aim of this work is to compare the performance of alternative metrics of anisotropy, both using simulated and experimental data.

Background

Geodesic Anisotropy (GeoA) was proposed by Batchelor in [4] and results from the redefinition of FA for a space of positive definite tensors. Ozarslan [5] introduced Generalised Anisotropy (GA) and Scaled Anisotropy (SE), calculated by fitting a *k*-rank tensor to the diffusion data (k = 2, 4, 6,…). Based on a metric for the shared diffusion anisotropy between two neighbouring voxels, Pipe [6] proposed a model free approach called GAA. The last metric to be considered in this study was proposed by Chen [7] and offers an information theoretical approach to characterization of anisotropy, based on the calculation of the cumulative residual entropy (CRE) [8] of the signal attenuation due to diffusion.

$$CNR = \frac{\overline{metric(fibre_1)} - \overline{metric(fibre_2)}}{\left(\sigma_1^2 + \sigma_2^2\right)^{1/2}} \quad (1)$$

Methods

Simulations: Contrast-to-noise ratio (CNR) (1) [2] is used here as our measure of the utility of a metric to distinguish between tissue types**.** Simulations were computed using 63 gradient directions and b-value=1000 s/mm^2. The noise-free diffusion weighted signals were calculated according to the diffusion tensor model [7]. Rician noise was then added to this data for different signal to noise ratios (SNRs). FA, GA2, GA4, GA6, SE2, SE4, SE6, GAA, and CRE were then estimated from this data. The procedure of noise generation and calculation of the metrics of anisotropy was repeated 40000 times in order to determine the mean and standard deviation of each metric, required for the calculation of CNR. The degree of anisotropy of the simulated fibres was characterized in terms of an anisotropy index defined for cylindrical symmetry, where two eigenvalues are equal (with value λ_2) and the third eigenvalue, λ_1, may be different: $A=(\lambda_1-\lambda_2)/(\lambda_1+2\lambda_2)=(\lambda_1/\lambda_{av}-1)/2$ and λ_{av} is the average of the three eigenvalues. In order to evaluate the performance of each metric for small anisotropy differences, we simulated fibres with λ_{av} =0.5, 0.7, 0.9 and 1.1×10^{-3}mm^2/s with A differences between $fibre_1$ and $fibre_2$ of 0.05. Large anisotropy differences were considered by keeping $A(fibre_1)$ constant and equal to 0.1, while increasing the anisotropy of $fibre_2$ in A increments of 0.05. All simulations were repeated with SNR=10, 25, 50 and 100 for the b=0 signals. Simulations were also repeated for 2, and 3 crossing fibres using a Gaussian mixture model to calculate the noise free signals.

Experimental data: Anisotropy maps of all metrics were obtained for a datasets of a healthy volunteer (voxel dimensions 2.0 x 2.0 x 2.0 mm^3) acquired with a Siemens 3T Tim Trio (63 directions as above). Four regions of interest (ROI) were drawn in brain regions were 1-fibre populations have been identified (corpus callosum – anterior and posterior – and cortico-spinal tract at the level of the internal capsule – left and right), and four more in 2-fibre population brain regions (intersection of radiations form the corpus callosum with the anterior part of corona radiata – left and right – and interfaces of optic radiations with tapetum and arcuate fasciculus – left and right). Six other ROIs of brain regions with significantly different anisotropies where also drawn, for the purpose of calculating the contrast-to-scatter ratio (CSR) (2) for the different metrics: cortical grey matter (GM), thalamus (TH), parasaggital white matter (PWM), pons (P), internal capsule (IC) and splenium (S). All ROIs were drawn in MNI space, and the anisotropy maps were transformed to this space using vtk.

$$CSR(metric) = \frac{\overline{metric(ROI_x)} - \overline{metric(ROI_y)}}{\left(\sigma_x^2 + \sigma_y^2\right)^{1/2}} \quad (2)$$

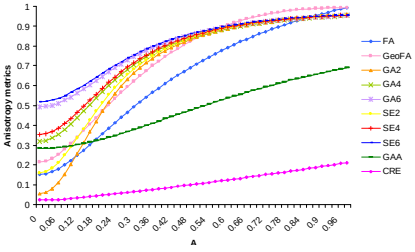

Fig. 1 – Profiles of anisotropy metrics as a function of *A*, SNR0=25.

Results and Discussion

Simulations: Fig. 1 shows the profiles of all the anisotropy metrics as a function of the simulated value of *A*. For one fibre simulations and small anisotropy differences between $fibre_1$ and $fibre_2$, GA and SE for a 2-rank tensor and CRE show higher CNR than FA, while the other metrics produced lower contrast-to-noise ratios. For large anisotropy differences, all metrics produce similar CNRs for anisotropy differences up to ΔA=0.4, but for larger anisotropies the CNR values for GA and SE (any rank) are significantly lower than what is observed for other metrics, and FA produces the best results.

FA shows the most significant drop in absolute value between 1 and 2 fibre compartments, showing a maximum drop of 44% for simulated values of *A* around 0.4. For a 2-fibre compartment, the values of CNR for small anisotropy differences show similar profiles to the ones observed for 1-fibre compartments with CRE producing the best results, but for large anisotropy differences FA, GeoA, CRE and GAA show significantly lower values than GA and SE, and GA produces the best results. When we simulate a 3-fibre compartment, only GAA, SE and GA (4- and 6-rank) can still differentiate this compartment from an isotropic one, with GA and SE for a 4-rank tensor showing the best performance.

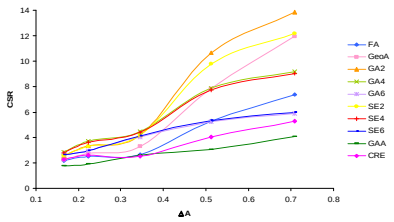

Fig. 2 – CSR profiles for six ROIs with different levels of anisotropy.

Experimental data: All metrics produced significantly higher values for the 1-fibre population ROIs when compared to the 2-fibre populations, but FA and CRE produced the most significant drops, with a maximum of 57.7% for FA and 61.0% for CRE. These values are higher than the ones observed for simulated data, but that can be explained if we take into consideration that with simulated data we were comparing the results obtained for compartments of one and two fibres with the same intrinsic anisotropy, which may not be the case in real data.

The profiles obtained for CSR with the six regions of interest considered (Fig. 2) are much closer to the profiles observed for CNR in a 2-fibre compartment, than to the profiles observed with 1-fibre simulations: GA2 and SE2 show the best overall results, followed by GA4 and SE4, while FA produces CSR values significantly lower; GeoA produces CSR values slightly higher than FA for low anisotropy differences, but for large anisotropy differences the CSR values observed for GeoA increase rapidly, as seen in 2-fibre simulations.

Conclusion

GeoA corresponds to a very elegant mathematical re-definition of FA [4], and it does show some improvement relatively to the traditional definition, for example by showing a smaller drop of values between 1 and 2-fibre populations. However, this framework depends on the diffusion tensor being positively defined, which is not always true in all regions of the brain (due to noise and inadequacy of the diffusion tensor model), and therefore this approach is only valid in regions of the brain where we have well defined 1-fibre populations. CRE and GAA do not show any advantages over FA. Finally, the use of a higher rank tensor results in increased ability to differentiate between tissues, both for simulated and experimental data. In addition, this model also produces a less significant drop between 1 and 2-fibre populations, and it is capable of identifying anisotropy in 3-fibre populations, and therefore affirming itself as a very promising approach.

References: **1.** Alexander *et al.* MRM 2000; 44:283-291. **2.** Kingsley and Monahan. MRM 2005; 53:911-918. **.** Jiun-Jie *et al.* JMRI 2006; 24:211-217. **4.** Batchelor *et al.* MRM 2005; 53:221-225. **5.** Ozarslan *et al.* MRM 2005; 53:866-876. **6.** Pipe and Farthing. MRI 2003; 49:536-542. **7.** Chen *et al.* IPMI 2005, LNCS 3565, pp. 246-257. **8.** Rao *et al.* IEEE Trans. Inf. Theory 2004; 50:1220-1228. **9.** Basser *et al.* JMR 1994; 103:247-254.